Journal of Basics and Applied Sciences Research (JOBASR)
ISSN (print): 3026-9091, ISSN (online): 1597-9962
Volume 2(4) December 2024
DOI: https://doi.org/10.33003/jobasr-2024-v2i4-64

Sol-Gel Derived Al:B:ZnO Thin Films: UV-Vis and PL Characterization for Solar Cell Applications

Yabagi Jibrin Alhaji [1], Ewansiha Kingsley Osarumwense[1,3]*, Ladan Muhammed Bello [1], Nmaya Mohammed Mohammed [1] and Kimpa Mohammed Isah [2]

[1]Department of Physics, Ibrahim Badamasi Babangida University, Lapai, Niger State.
[2]Department of Physics, Federal University of Technology Minna, Niger State
[3]Department of Physics, Federal Polytechnics Bida, Niger State
*Corresponding Author Email: kingsleyewansiha74@gmail.com

Keywords:
Zinc oxide (ZnO),
solar cells,
Broron,
Aluminuim.

ABSTRACT
This study investigates the effects of co-doping ZnO thin films with aluminum (Al) and boron (B) on their optical properties for enhanced solar cell efficiency. Using the Sol-gel synthesis process, we deposited ZnO thin films with varying Al and B precursor concentrations (1-4 wt%) on glass substrate via dip-coating. UV-visible and photoluminescence (PL) spectroscopy characterized the films' optical characteristics. The results show that co-doped ZnO films exhibit high transparency (up to 91%) and tunable band gaps (3.1-3.48 eV). Notably, the PL intensity (1.094) is significantly enhanced compared to singly doped ZnO:Al and ZnO:B, indicating optimized charge carrier dynamics. These findings demonstrate the potential of Al and B co-doped ZnO thin films for improved solar cell performance.

INTRODUCTION

One practical way to effectively transform solar energy into electrical power is to employ photovoltaic systems. This is made possible by solar cells, a key component of this process (Pastuszak & Wgierek, 2022). The first generation of solar cells were made using silicon (Si), which was originally the most widely utilized material in the absorber layer of solar cells, especially on an industrial scale. However, more recent studies have found that other materials, like cadmium telluride (CdTe) and copper indium gallium selenide (CIGSe), have better fundamental qualities than Si. Doroody et al. (2022) claim that these materials are thinner (between 13 m thickness), have a larger absorption coefficient (105 cm^{1}), an adjustable band gap, and possibly even some flexibility. In order to minimize energy losses, it is crucial to ensure that sunlight enters the absorber layer properly and that the generated charges are collected successfully, especially in the presence of materials other than silicon (Regmi et al.,2023).This necessitates the employment of an effective transparent conductive oxide(TCO), often constructed of oxide minerals. Due to its increased conductivity and transparency under visible light when created in thin film form, TCO coatings have a significant potential usage in photovoltaic and transparent electronics applications (Gultepe & Atay, 2022). There are numerous significant uses for TCOs. They are frequently used as electrical contacts for light-emitting diodes and solar cells due to their unusual combination of electrical conductivity and optical transparency (Chavan et al., 2023). Indium tin oxide (ITO) and fluorine-doped tin oxide (FTO) are the two forms of TCO that are most commonly utilized in industries. The TCO is the most often utilized top layer in thin film solar cells because of its exceptional conductivity and transparency (Faremi et al., 2022). ITO exhibits both transparency and low thickness-dependent resistance. However, the expensive cost, possible health risks, and difficulties in using fluorine in FTO deposition related to indium have necessitated the need for alternative TCO materials. In an ideal world, alternatives to transparent conducting layers and electrodes would include stable electrical conductivity under bending and stretching pressures, flexible, eco-friendly, and heat-efficient to construct. As a viable alternative to ITO, zinc oxide is a promising possibility (Koralli et al., 2022).Different nanomaterials have different properties that make them suitable for solar cells. Different isolated solar cell layers have been created us ing a variety of materials.One of the most fascinating materials to have undergone extensive research has been zinc oxide.

Due to its nontoxicity and stable wurtzite structure with lattice spacing of a=0325nm and b=0.521nm, zinc oxide (ZnO) is a very promising material for solar cell applications (Shweta & Thapa, 2019).

Zinc oxide (ZnO) is one of the most studied semiconductor oxides because of its numerous beneficial and attractive properties, such as its excellent chemical and thermal stability and lack of toxicity.Zinc oxide (ZnO) is a practical and reasonably priced semiconductor with a wide direct band gap that finds application in a wide range of scientific and technological domains (Amakali et al., 2020). The nano size ZnO has various applications like UV nano-lasers, nano-generators, gas sensors, biosensors, solar cells, photo detectors, photo catalysts and surface acoustic wave devices due to its unique and superior physical and chemical properties(Shweta & Thapa, 2019). ZnO powder with other materials has been used to produce batteries, ferrites, ceramics, glass, cement, lubricants, paints, adhesives, plastics, sealants, and food nutrients (Orori, 2023). This research shall emphasis on preparation, synthesis, and characterization of Aluminuim and Boron thin films co-doped with Zinc oxide (A: B: ZnO) using dip- coating techniques of sol-gel method for application in solar collectors as window layers of solar cells. The sol-gel method involves the conversion of a precursor solution (sol) into a solid metal oxide film (gel) through hydrolysis and condensation reactions. It offers flexibility in film composition and can be used with various metal oxide materials. Sol-gel deposition can be performed using spin coating, dip coating, or other techniques. It allows for low-temperature processing and is suitable for a wide range of substrates (Bokov et al., 2021). The sol-gel method has gained much interest among researchers as it offers controlled consolidation, shape modulation, patterning of the nanostructures and low processing temperature (Gultepe & Atay, 2022). It comprises the condensation, hydrolysis, and thermal decomposition of metal alkoxides or metal precursors in solution. A stable solution is formed, known as the sol. Upon hydrolysis or condensation, the gel is formed with increased viscosity. The particle size can be monitored by changing precursor concentration, temperature, and pH values. A mature step is mandatory to empower the development of solid mass it may take a few days in which the removal of the solvent, Ostwald ripening, and phase alteration could happen. The unstable reagents are detached to produce nanoparticles (Li et al., 2019). The focus of the research is to vary the precursor concentration of ZnO, Al and B while they are being co-doped. ZnO co-doped with Al and B can be enhanced by increasing the carrier mobility and concentration. According to Lee et al. (2016), B functions as an acceptor, making up for the donor-like flaws, while Al acts as a donor, adding extra electrons. The transparency in the visible and near-infrared spectrums can also be improved by co-doping Al and B with ZnO. According to Chen et al. (2015), this is because flaws and contaminants scatter light less. The optical and electrical characteristics can be improved by co-doping ZnO with Al and B, it has the ability to lower the defect density. Defects such as oxygen vacancies and zinc interstitials can be passivated by Al and B (Wang et al., 2016). Co-doping Al and B can also tune the ZnO bandgap. The bandgap can be altered to suit a variety of applications by varying the concentrations of Al and B (Kim et al. 2017). ZnO stability can be enhanced by co-doping with Al and B under a variety of environmental circumstances. ZnO's reactivity can be decreased by Al and B, increasing its resistance to degradation (Lee et al., 2018). The A:B:ZnO nanoparticles produced shall be characterize by Photoluminescence (PL) and UV- Visible Spectroscopy (UV-Vis). The concentration of each dopant will be varied to ascertain the correct percentage for maximum efficiency performance of solar cells. Therefore we aimed to ascertain a precursor concentration and bandgap for ZnO co-doped with Al and B that will give a low absorption and high transmittance for window layer of solar cell compared to existing research results.

MATERIALS AND METHODS

Approach to Conducting the Literature Review:

Varied concentration of Zinc acetate dihydrate ($Zn(CH_3CO_2)_2.2H_2O$) (1g, 3g, 5g) was dissolved in 50 ml of 2-methoxyethanol ($(CH_3)_2CHOH$, Aldrich, 99.8%), and rapidly agitated with a magnetic stirrer at room temperature for 15 minutes according to (Bouacheria et al., 2022). As a stabilizer, monoethanolamine (MEA: $H_2NCH_2CH_2OH$, Aldrich, 99.5%,) was added drop-wise while stirring continuously at a molar ratio of 1:1 in the MEA mixture as adopted by Saleem *et al*., (2012). After an hour of stirring at 60˚C, the resulting solution became clear and uniform, ready for coating. To guarantee that a homogenous, transparent solution is produced, the resultant mixture was further agitated for 40 minutes. After that, the mixture was centrifuged at 3500 rpm to get rid of the unreacted components. (Musleh *et al*., 2018) and then filtrated by using the standard 0.45µm filter paper as adopted by(Alsaad et al., 2020). The next stage was the Preparation of Al – doped ZnO (A:ZnO) and B- doped ZnO (B:ZnO) Solutions The process involved incorporating varied concentration of boric acid (H_3BO_3) (1%, 2%, 3% and 4%) into the ZnO solution to create B:ZnO and varied concentration of aluminum nitrate ($Al(NO_3)_39H_2O$) (1%, 2%, 3% and 4%) into the ZnO solution to create A:ZnO accordingly. Using a magnetic stirrer for two hours at 60 ^{O}C, a transparent solution for each of the doped systems was created. Lastly, 0.45µm filter paper was used to filter the resultant solution. At room

temperature, the corresponding solution was swirled for two hours at 60 ^{O}C. This procedure was followed strictly to ensure the creation of solutions that can maintain a high degree of transparency. To prepare the A:B:ZnO both solutions were combined. For hydrolysis and condensation, the corresponding solution was stirred for two hours at room temperature at 60 ^{O}C. To allow for the aging process, the colorless, transparent, homogenous solution was being kept at room temperature for a full day. Following the preparation of the solutions with the required characteristics, the glass substrate was dipped in the sol and removed using the dip-coating process at the rate of 0.9cm/min in room temperature for three hours.This method enabled the production of thin films with an average thickness of 300 nm. After that, the produced films were dried in an oven for 15-20 minutes at 200 to 300 ^{O}C in order to remove the solvent and any polluted organic residues. For the organics to completely evaporate and for the ZnO film to begin forming and crystallizing, the temperature of the preheat treatment is very necessary. This process was followed by annealing in air at a temperature of 500 ^{O}C for two hours(Stroescu et al., 2023).

Table 1: Precusor Concentration

RUNS	PRECUSOR CONCENTRATION(g) SAMPLE A ZnO:A:B	PRECUSOR CONCENTRATION(g) SAMPLE B ZnO:A:B	PRECUSOR CONCENTRATION(g) SAMPLE C ZnO:A:B
1	1g(1%)(1%)	3g(1%)(1%)	5g(1%)(1%)
2	1g(2%)(2%)	3g(2%)(2%)	5g(2%)(2%)
3	1g(3%)(3%)	3g(3%)(3%)	5g(3%)(3%)
4	1g(4%)(4%)	3g(4%)(4%)	5g(4%)(4%)

RESULTS AND DISCUSSION

Uv-Vis Spectroscopy

Ultraviolet visible, or UV-Vis, spectroscopy is widely utilized to furnish characterization information for a range of materials. The fundamental idea of UV-visible spectroscopy is that different spectra are produced when chemical compounds absorb ultraviolet or visible light. UV-Vis spectroscopy can be used to characterize a wide variety of materials. The UV-Vis provides information based on sample responses and the degree of transmittance or absorption of a range of beam light wavelengths. Wavelengths between 200 and 700 nm are commonly used to characterize metal and metal oxide nanoparticles (Abhishek et al., 2023). We have used the UV-Vis spectra to characterize the 12 ZnO:Al:B samples. The wavelengths were plotted against the absorbance levels, as seen in Figures 1 through 4.

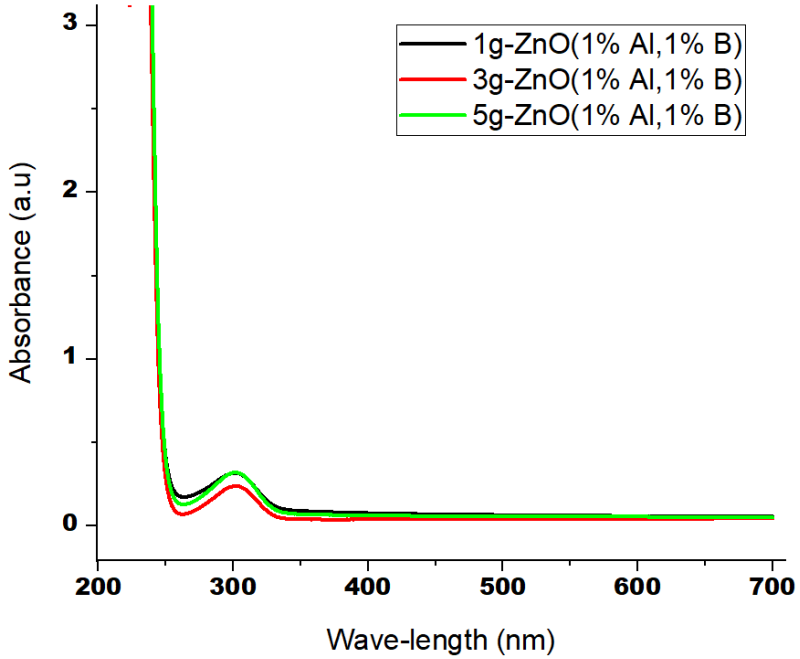

Figure 1: UV-Vis Spectra for Run 1

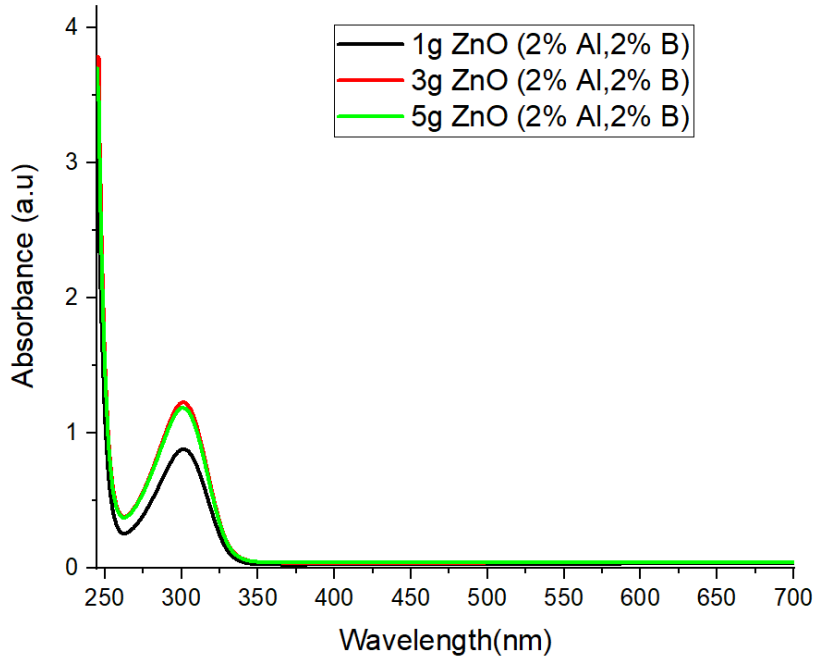

Figure 2: UV-Vis Spectra for Run 2

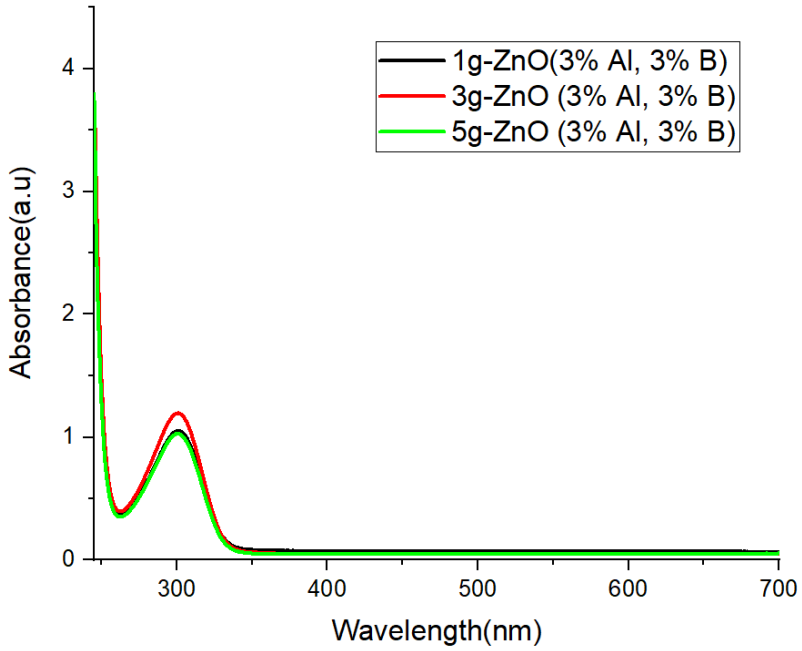

Figure 3: UV-Vis Spectra for Run 3

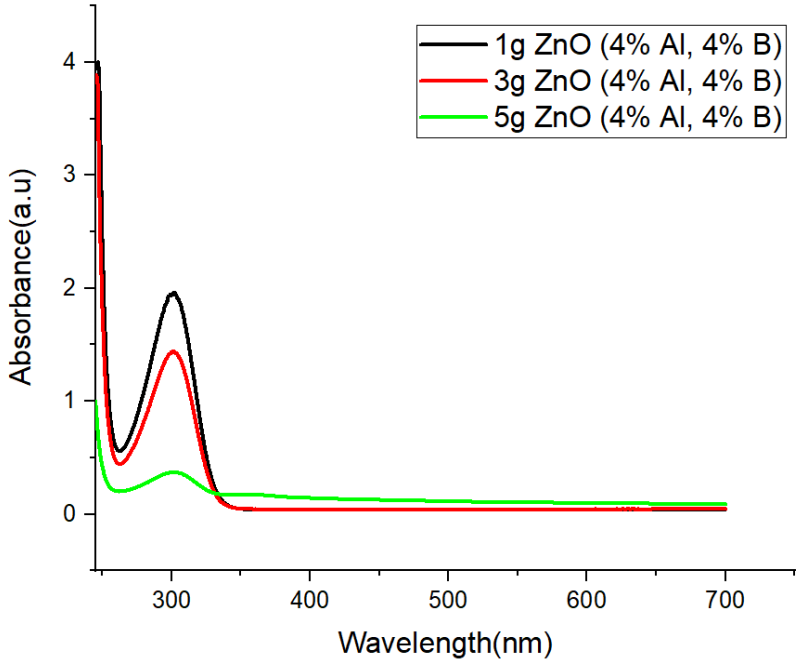

Figure 4: UV-Vis Spectra for Run 4

Determination of the Bandgap energy (Eg)

The band gap value of ZnO:A:B was ascertained using the Tauc plot and the data from UV-Vis measurements that were acquired for all the runs. A Tauc plot is a graphical representation of the optical absorption properties of a material, used to determine the bandgap energy (Eg) (Makuła et al., 2018). A plot of variation of $(\alpha h\nu)^{1/2}$ versus hν for all the samples are shown in Fig 5 through Fig 8 The band gap energy is obtained by extrapolating the straight line portion of the plot to zero. The presence of a single slope in the plot suggests that the films have direct and allowed transition(Khan et al., 2011).

The calculations are governed by the following formulas (Akhta et al., 2013);

Tauc Relation

$$\alpha(h\nu) = A(h\nu - Eg)^n \quad (1)$$

Where α is absorption coefficient, v is speed of light, A is absorbance, Eg is bandgap energy and since zinc oxide is a direct bandgap semiconductor, so it exhibits a direct transition, n=1/2.

The Beer- Lambert Law or absorption coefficient formula

$$A\ (cm^{-1}) = \frac{2.303 \times A}{d} \quad (2)$$

Where d is the thickness of the film (cm) and A is the absorbance (unitless)

The Beer- Lambert Law, named after August Beer and johann Heinnrich Lambert, describes the relation between absorbance, concentration and path length. The constant 2.303 arises from 2.303 = In (10)

where In is the natural logarithm

The Energy- Wavelength Conversion Formula

$$E\ (eV) = \frac{1240}{\lambda\ (nm)} \quad (3)$$

The formula converts the wavelength (λ) of light (in nanometers, nm) to photon energy (E) in electronvolts (eV).

1240 is a constant derived from 1240eV nm = hv/e

Where h is Plank's constant (6.626 x 10^{-34} Js), c is speed of light (3 x $10ms^{-1}$) and e is elementary charge (1.602 x 10^{-19} C)

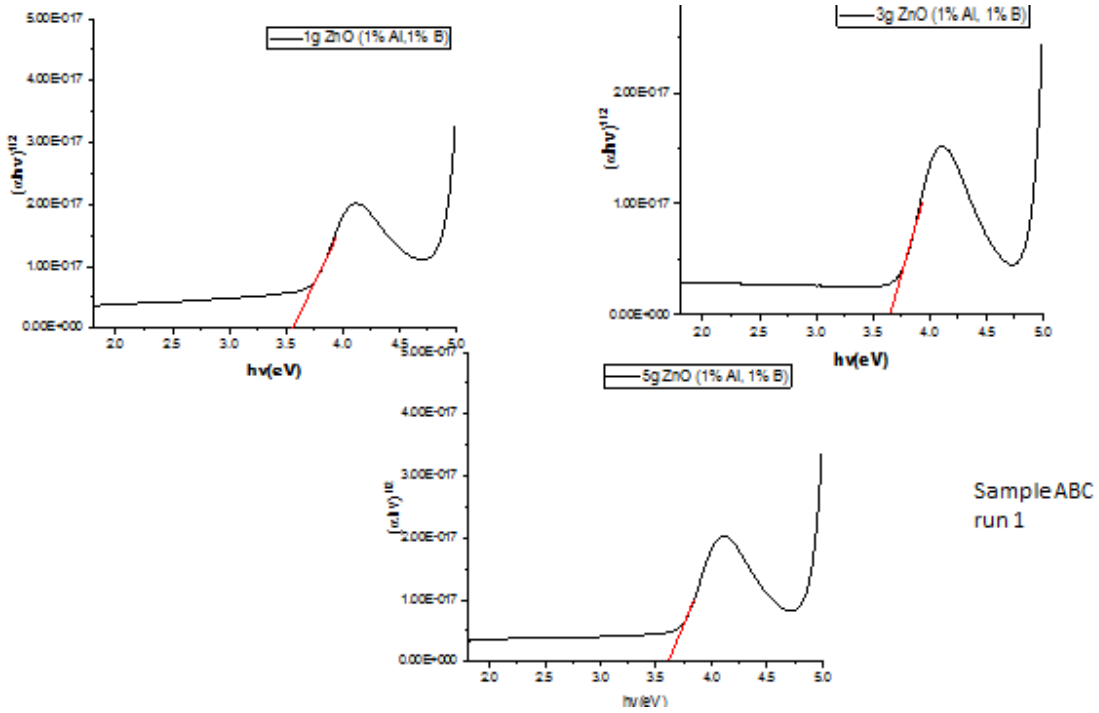

Figure 5: Tauc plots for Run 1

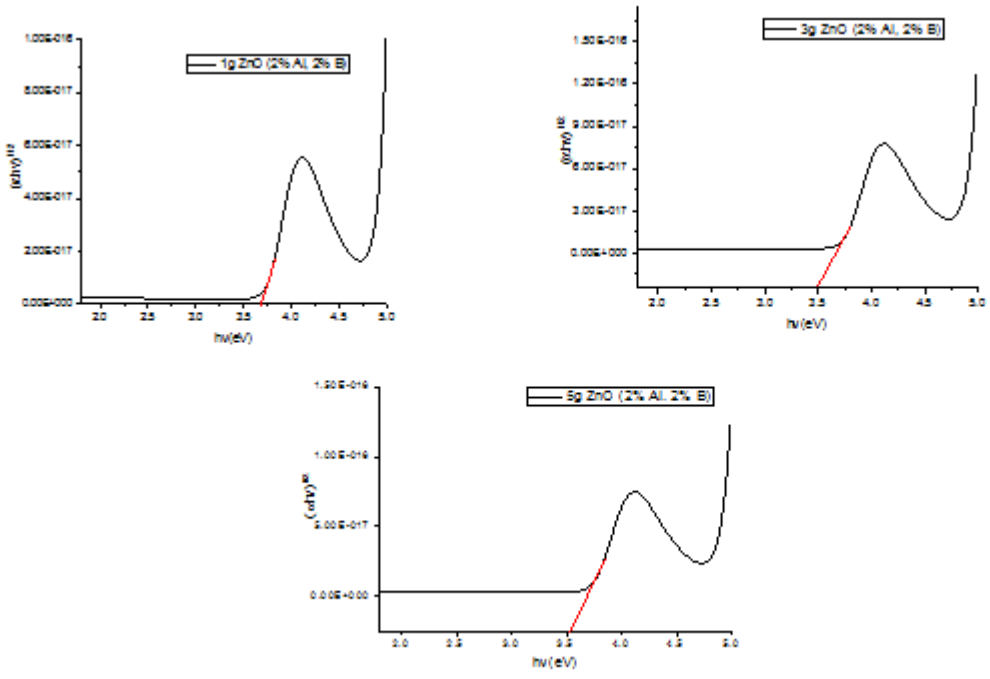

Figure 6: Tauc plots for Run 2

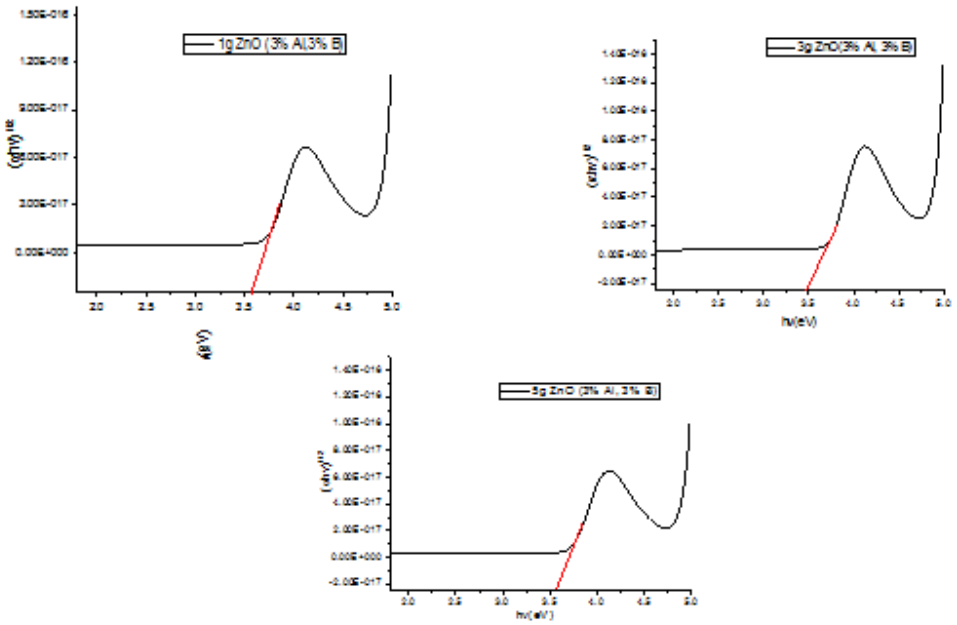

Figure 7: Tauc plots for Run 3

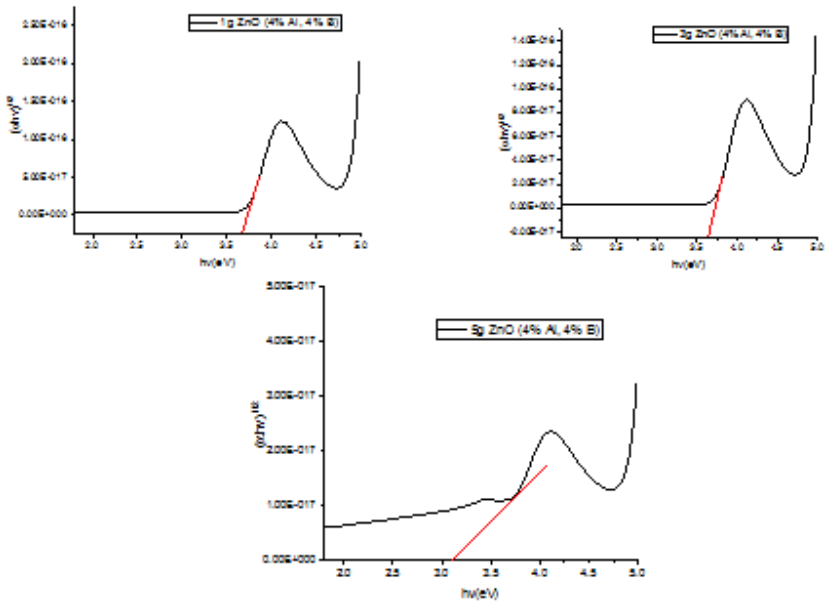

Figure 8: Tauc plots for Run 4

Table 2: Energy Bandgap (eV) for doped ZnO nanoparticles

Run	Sample	Bandgap (eV)
1	A	3.55
	B	3.65
	C	3.62
2	A	3.68
	B	3.49
	C	3.53
3	A	3.57
	B	3.47
	C	3.56
4	A	3.67
	B	3.63
	C	3.1

Generally speaking, optical constants refer to two of the most significant optical characteristics: the extinction coefficient and the refractive index. Light transmission through thin-film material is dependent on the quantity of absorption and reflection that occurs along the light path(Govindasamy et al., 2016).

We are going to calculate the extinction coefficient , refractive index and electrical susceptibility of run 2 sample C which corresponds to Zno:A:B (5g(2%)(2%)). This particular thin- film was chosen because it has the best bandgap for window layer of solar cell and a good transmittance of 90%. The absorbance for the transmittance is 0.045 and it falls between wavelength ranges of 365 – 381nm.

Extinction coefficient (k) (Govindasamy et al., 2016)

$$k = \frac{\lambda \times A}{4 \times \pi \times d} \quad (4)$$

Where λ is wavelength (365nm), A is absorbance (0.045) and d is is the film thickness (50nm). From the equation above k is 0.00258

Refractive index (n)

Using the Kramers-Kronig relation(Salwan K. Al-Ani, 2008)

$$n = \sqrt{\frac{1+(2\times\eta)}{(1-\eta)}} \quad (5)$$

Where η is reflectance (related to absorbance)

Approximating η from absorbance

$$\eta = \frac{A}{(2\times log10(e))} \quad (6)$$

η = 0.0196

From equation

n = 1.994

The values of the extinction coefficient (0.00258) and the refractive index (1.994) are very suitable for window layer of solar cell.

Electrical susceptibility

To calculate the electrical susceptibility (χe) we use

$$\chi e = \varepsilon r - 1 \quad (7)$$

Where εr is relative permittivity (dielectric constant)

$\varepsilon r = n^2$

εr = 3.976

Therefore χe is 2.976

The UV-Vis results obtained for run 2 sample C which corresponds to Zno:A:B (5g(2%)(2%)) shows Bandgap energy (Eg) of 3.53 eV, which is consistent with previous reports on Al and B co-doped ZnO thin films (Mahmood & Naeem, 2017). The large bandgap which is greater than that of Bulk ZnO (3.37 eV) can be attributed to the co- doping with Al and B which are due to quantum confinement effect of the ZnO nanoparticles (Alsaad et al., 2020). The larger optical bandgaps of the ZnO thin film maybe due to high crystalline quality(Akhta et al., 2013). The extinction coefficient (k): 0.00258, indicating low absorption and high transparency, in agreement with studies on ZnO thin films (Sharmin et al., 2019). The Refractive index (n): 1.994, comparable to reported values for ZnO thin films (Stroescu et al., 2023) is very good for window layer of solar cell.Transmittance: 90%, demonstrating high optical transparency, suitable for window layer applications (Bin Rafiq et al., 2020).Electrical susceptibility: 2.976, indicating a moderate response to electromagnetic fields.Zhang et al. (2011) reported a bandgap energy of 3.31 eV for Al and B co-doped ZnO thin films.Rakhshani et al. (2009) achieved a transmittance of 82% for similar co-doped ZnO thin films.(Nagayasamy et al., (2013) obtained an extinction coefficient of 0.003 for ZnO thin films.

Photoluminescence (PL) of ZnO:Al, ZnO:B and ZnO:Al:B

The PL spectra of ZnO:Al, ZnO:B, and ZnO:Al:B, each exhibiting distinct optical activity based on doping with aluminum (Al), boron (B), and a

combination of both Al and B are presented in Fig. 9. The PL spectrum of ZnO doped with Al shows a peak at a wavelength of 370.56 nm with an intensity of 0.278. The emission near the ultraviolet (UV) region corresponds to the near-band-edge (NBE) emission of ZnO, which is characteristic of excitonic recombination processes, that is, the recombination of electrons and holes at the conduction and valence bands. The slight blue shift observed in the wavelength (compared to the pure ZnO peak, typically around 378–380 nm) is attributed to the incorporation of Al^{3+} ions into the ZnO lattice. Al doping introduces donor states within the ZnO matrix, contributing to enhanced free electron concentration. This increase in carrier density results in a Burstein-Moss shift, wherein the Fermi level moves into the conduction band, effectively widening the band gap. As a result, the wavelength of emission decreases slightly, as seen in the blue shift. Asvarov*et al.* (2022) found that increasing Al doping levels led to a broadening and suppression of the PL peak, indicating deterioration in crystalline quality, which aligns with the theoretical expectations of increased free carrier concentration. Tuan (2023) observed that the PL spectra of ZnO nanoparticles exhibited a strong UV emission peak, attributed to excitonic recombination, which is enhanced by the presence of Al dopants. The intensity of 0.278 suggests that Al doping enhances the recombination of excitons. This moderate intensity reflects that while Al doping improves the optical response, it does not introduce significant defects that could further alter the PL characteristics.

Boron doping in ZnO, represented by the ZnO:B spectrum, shows an emission peak at 372.50 nm with an intensity of 0.171 (Fig. 7b). This peak is slightly red-shifted compared to ZnO:Al, indicating a narrowing of the band gap, which is expected when a dopant like B is incorporated. B^{3+} ions, which have a smaller ionic radius than Zn^{2+}, create localized states in the band structure, potentially acting as acceptor states. This leads to a reduction in the effective band gap, hence the observed red shift in the emission wavelength. The intensity of the PL peak is lower for ZnO:B (0.171) compared to ZnO:Al (0.278). This reduction in intensity may be attributed to the increased non-radiative recombination processes in ZnO:B. Boron doping is known to introduce more defect states, particularly oxygen vacancies and zinc interstitials, which serve as centers for non-radiative recombination. This defect formation can significantly impact the PL characteristics, as defects can trap charge carriers and facilitate non-radiative recombination pathways, thereby diminishing the overall PL intensity (Khalid *et al.*, 2022; Üzar, 2024). These defects capture free electrons or holes, reducing the likelihood of radiative recombination and thus lowering the overall PL intensity. The red shift and decreased intensity in ZnO:B suggest that while boron doping modifies the electronic structure, it also introduces defect states that diminish the material's optical activity.

The PL spectrum of the co-doped ZnO:Al:B reveals a peak at 369.08 nm with a much higher intensity of 1.094. The PL spectrum shows dominant NBE emission between 360 to 380 nm which is a sign of improved crystal quality. Also, the ions of Al and B can occupy different lattice sites, reducing defeats and increasing crystal qualities. The emission at 369.08 nm represents the highest degree of blue shift among the samples, indicating that the co-doping of Al and B significantly alters the band structure. The pronounced blue shift can be explained by the synergistic effect of both dopants, where Al contributes to the Burstein-Moss effect by increasing the carrier concentration, and B modifies the band structure by introducing acceptor states. The result is a material with an even larger apparent band gap compared to the singly doped samples. The high PL intensity (1.094), which is substantially higher than both ZnO:Al and ZnO:B suggests that co-doping with both Al and B optimizes the charge carrier dynamics, enhancing the radiative recombination rate. This could be as a result of the introduction of both dopants reduces the overall density of defect states that promote non-radiative recombination. Al doping introduces donor levels that increase electron concentration, while B doping may create localized states that capture holes, facilitating enhanced excitonic recombination. This balance of donor and acceptor states likely leads to the significantly improved PL intensity. This is evident in the work of Tanaka (2024), where the dependence of PL on Al doping levels in 4H-SiC was explored, revealing significant peaks associated with Al-bound excitons at low temperatures, indicating enhanced carrier recombination due to increased electron availability. The blue shift in the ZnO:Al:B spectrum, in conjunction with the high PL intensity, suggests that this co-doped material exhibits superior optical properties, making it a promising candidate for optoelectronic applications. The enhanced radiative recombination and reduced non-radiative pathways highlight the advantage of co-doping, where the combined effects of Al and B lead to improved optical activity and greater emission efficiency. The NBE of 360 to 380nm for the ZnO:A:B indicates efficient emission and reduced non- radiative recombination. The emission agrees with energy range foe photovoltaic applications. A strong PL response is widely regarded as an indicator of a high-quality surface, and PL measurements are nondestructive and environment insensitive (Gfroerer, 2006).

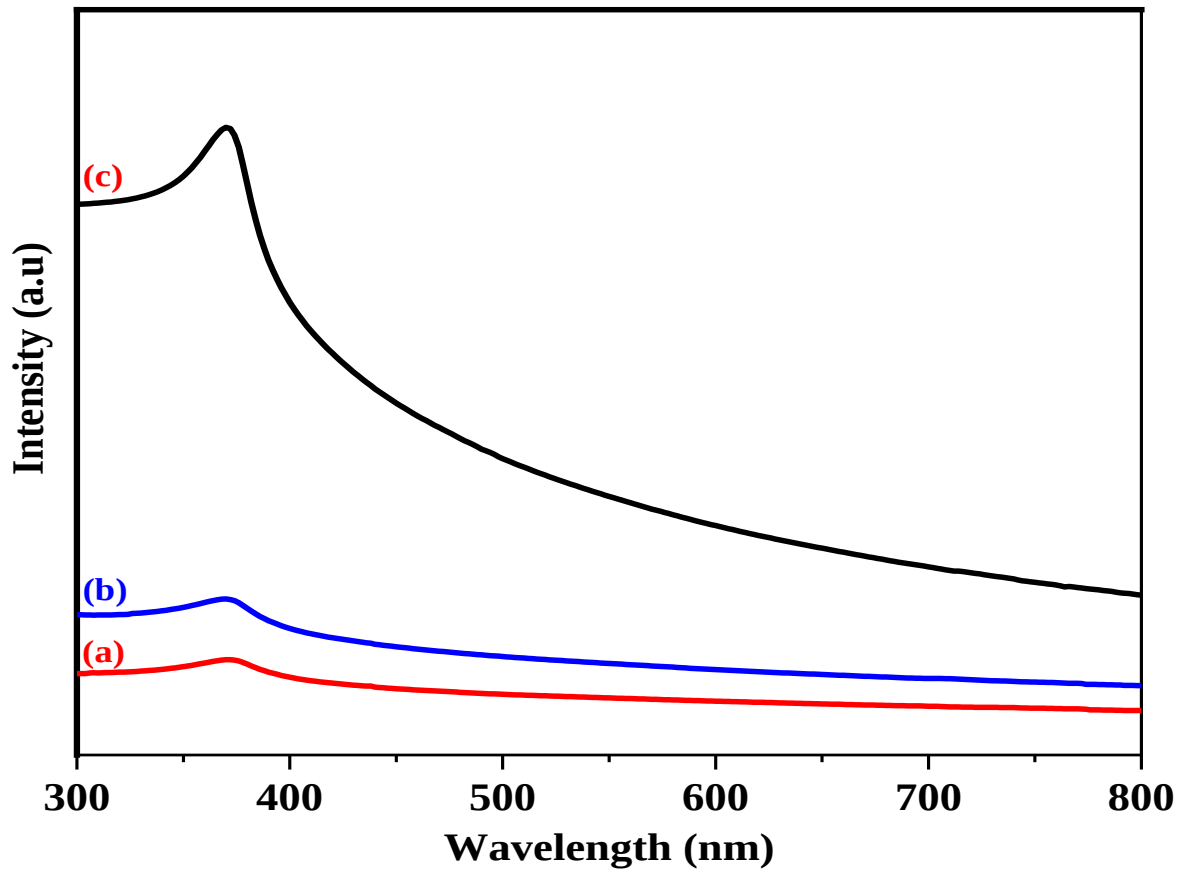

Figure 9: PL spectra of (a) ZnO:B (b) ZnO:Al (c) ZnO:Al:B

CONCLUSION

This study explored the optical properties of ZnO precursors co-doped with aluminum (Al) and boron (B) at varied concentrations, revealing their potential as high-efficiency window layers in solar cells. Notably, the estimated bandgap energy (Eg) range of 3.10-3.48 eV, coupled with a maximum transmittance of 91%, confirms ZnO's suitability for photovoltaic applications.

The co-doped ZnO:Al:B exhibited enhanced optical activity, marked by a blue-shifted emission peak at 369.08 nm and a substantial increase in photoluminescence (PL) intensity (1.094). By reducing defect states and encouraging radiative recombination, this synergistic Al and B doping impact improved charge carrier dynamics. These results highlight ZnO:Al:B's promise for optoelectronic uses, especially in solar cells, where efficiency can be greatly increased by its blue-shifted emission, high PL intensity, and fewer non-radiative recombination routes.

REFERENCE

Abhishek, B., Shubhada, B., RaviKumar, M., Nandkishor, D., Shankar, B. (2023). Study of UV-Visible Spectroscopy. *International Journal of Research Publication and Reviews*, *04*(04),1140–1146. https://doi.org/10.55248/gengpi.2023.4149

Akhta, M. S., Riaz, S., Noor, R., & Naseem, S. (2013). Optical and structural properties of ZnO thin films for solar cell applications. *Advanced Science Letters*, *19*(3), 834–838. https://doi.org/10.1166/asl.2013.4822

Alsaad, A. M., Ahmad, A. A., Qattan, I. A., Al-Bataineh, Q. M., & Albataineh, Z. (2020). Structural, optoelectrical, linear, and nonlinear optical characterizations of dip- synthesized undoped zno and group iii elements (B, al, ga, and in)-doped zno thin films. *Crystals*, *10*(4). https://doi.org/10.3390/cryst10040252

Amakali, T., Daniel, L. S., Uahengo, V., Dzade, N. Y., & Leeuw, N. H. De. (2020). Structural and Optical Properties of ZnO Thin Films Sol – Gel Methods. *Crystals*, *10(2)*, 132.

Asvarov, A. S., Abduev, A. K., Akhmedov, A. K., & Kanevsky, V. M. (2022). On the Effect of the Co-Introduction of Al and Ga Impurities on the Electrical

Performance of Transparent Conductive ZnO-Based Thin Films. *Materials*, *15*(17), 5862.

Bin Rafiq, M. K. S., Amin, N., Alharbi, H. F., Luqman, M., Ayob, A., Alharthi, Y. S., Alharthi, N. H., Bais, B., & Akhtaruzzaman, M. (2020). WS2: A New Window Layer Material for Solar Cell Application. *Scientific Reports*, *10*(1), 1–11. https://doi.org/10.1038/s41598-020-57596-5

Bokov, D., Turki Jalil, A., Chupradit, S., Suksatan, W., Javed Ansari, M., Shewael, I. H., Valiev, G. H., & Kianfar, E. (2021). Nanomaterial by Sol-Gel Method: Synthesis and Application. *Advances in Materials Science and Engineering*, *2021*. https://doi.org/10.1155/2021/5102014

Bouacheria, M. A., Djelloul, A., Adnane, M., Larbah, Y., & Benharrat, L. (2022). Characteristics of ZnO and Al Doped ZnO Thin Films Prepared by Sol Gel Method for Solar Cell Applications. *Journal of Inorganic and Organometallic Polymers and Materials*, *32*(7), 2737–2747. https://doi.org/10.1007/s10904-022-02313-0

Chavan, G. T., Kim, Y., Khokhar, M. Q., Hussain, S. Q., Cho, E. C., Yi, J., Ahmad, Z., Rosaiah, P., & Jeon, C. W. (2023). A Brief Review of Transparent Conducting Oxides (TCO): The Influence of Different Deposition Techniques on the Efficiency of Solar Cells. *Nanomaterials*, *13*(7). https://doi.org/10.3390/nano13071226

Chen, X., Wang, Z., Li, M., Liu, Y., & Shen, D. (2015). Enhanced transparency and conductivity of ZnO:Al:B thin films. Journal of Materials Science: Materials in Electronics, 26(10), 8336-8342.

Doroody, C., Rahman, K. S., Kiong, T. S., & Amin, N. (2022). Optoelectrical impact of alternative window layer composition in CdTe thin film solar cells performance. *Solar Energy*, *233*(February), 523–530. https://doi.org/10.1016/j.solener.2022.01.049

Faremi, A. A., Akindadelo, A. T., Adekoya, M. A., Adebayo, A. J., Salau, A. O., Oluyamo, S. S., & Olubambi, P. A. (2022). Engineering of window layer cadmium sulphide and zinc sulphide thin films for solar cell applications. *Results in Engineering*, *16*(July), 100622. https://doi.org/10.1016/j.rineng.2022.100622

Gfroerer, T. H. (2006). Photoluminescence in Analysis of Surfaces and Interfaces. *Encyclopedia of Analytical Chemistry*, *February*. https://doi.org/10.1002/9780470027318.a2510

Govindasamy, G., Murugasen, P., & Sagadevan, S. (2016). Investigations on the Synthesis, Optical and Electrical Properties of TiO2 Thin Films by Chemical Bath Deposition (CBD) method. *Materials Research*, *19*(2), 413–419. https://doi.org/10.1590/1980-5373-MR-2015-0411

Gultepe, O., & Atay, F. (2022). Al and B co-doped ZnO samples as an alternative to ITO for transparent electronics applications. *Journal of Materials Science: Materials in Electronics*, *33*(18), 15039–15053. https://doi.org/10.1007/s10854-022-08421-4

Lee, J., Lee, S., Kim, H., Kim, D., and Kim, Y. (2016). Synergistic effects of Al and B co- doping on the electrical and optical properties of ZnO thin films. Journal of Alloys and Compounds, 688, 101-106.

Lee, J., Lee, S., Kim, H., Kim, D., & Kim, Y. (2018). Improved stability of ZnO:Al:B thin films under environmental stress. Journal of Materials Science: Materials in Electronics, 29(10), 8336-8342.

Li, Y., Cheng, M., Jungstedt, E., Xu, B., Sun, L., & Berglund, L. (2019). Optically Transparent Wood Substrate for Perovskite Solar Cells. *ACS Sustainable Chemistry and Engineering*, *7*(6), 6061–6067. https://doi.org/10.1021/acssuschemeng.8b06248

Khan, Z. R., Khan, M. S., Zulfequar, M., & Shahid Khan, M. (2011). Optical and Structural Properties of ZnO Thin Films Fabricated by Sol-Gel Method. *Materials Sciences and Applications*, *02*(05), 340–345. https://doi.org/10.4236/msa.2011.25044

Khalid, A., Ahmad, P., Muhammad, S., Khan, A., Khandaker, M.U., Alam, M.M., Asim, M., Din, I.U., Iqbal, J., Rehman, I.U. and Razzaq, Z., 2022. Synthesis of boron-doped zinc oxide nanosheets by using phyllanthus emblica leaf extract: a sustainable environmental application. *Frontiers in Chemistry*, *10*, p.930620.

Kim, H., Kim, D., Kim, Y., Lee, S., & Lee, J. (2017). Tunable bandgap of ZnO:Al:B thin films by adjusting the Al and B concentrations. Journal of Alloys and Compounds, 722, 811-816.

Koralli, P., Varol, S. F., Mousdis, G., Mouzakis, D. E., Merdan, Z., & Kompitsas, M. (2022). Comparative Studies of Undoped/Al-Doped/In-Doped ZnO Transparent Conducting Oxide Thin Films in Optoelectronic Applications. *Chemosensors*, *10*(5). https://doi.org/10.3390/chemosensors10050162

Mahmood, A., & Naeem, A. (2017). Sol-Gel-Derived Doped ZnO Thin Films: Processing, Properties, and Applications. *Recent Applications in Sol-Gel Synthesis*.

https://doi.org/10.5772/67857

Makuła, P., Pacia, M., & Macyk, W. (2018). How To Correctly Determine the Band Gap Energy of Modified Semiconductor Photocatalysts Based on UV−Vis Spectra. *Journal of Physical Chemistry Letters*, *9*(23), 6814–6817. https://doi.org/10.1021/acs.jpclett.8b02892

Musleh, H., AlDahoudi, N., Zayed, H., Shaat, S., Tamous, H. M., Shurrab, N., Issa, A., & Asad, J. (2018). Synthesis and Characterization of Zno Nanoparticles Using Hydrothermal and Sol-Gel Techniques for Dye-Sensitized Solar Cells. *Journal of University of Babylon for Engineering Sciences*, *26*(9), 256–267. https://doi.org/10.29196/jubes.v26i9.1736

Nagayasamy, N., Gandhimathination, S., & Veerasamy, V. (2013). The Effect of ZnO Thin Film and Its Structural and Optical Properties Prepared by Sol-Gel Spin Coating Method. *Open Journal of Metal*, *03*(02), 8–11. https://doi.org/10.4236/ojmetal.2013.32a2002

Orori, M. C. (2023). *Properties of Zinc Oxide thin layers for Photovoltaic Applications*. *7*(3), 1–9. https://doi.org/10.19080/JOJMS.2023.07.555716

Pastuszak, J., & Węgierek, P. (2022). Photovoltaic Cell Generations and Current Research Directions for Their Development. *Materials*, *15*(16). https://doi.org/10.3390/ma15165542

Rakhshani, A. E., Makdisi, Y. and Ramazaniyan, H. A. (2009) "Effects of Al doping on the structural and optical properties of ZnO thin films," Journal of Alloys and Compounds, 484(2), 434-438.

Regmi, G., Rijal, S., & Velumani, S. (2023). Aluminum-doped zinc oxide (AZO) ultra-thin films deposited by radio frequency sputtering for flexible Cu (In , Ga) Se 2 solar cells. *Memories - Materials, Devices, Circuits and Systems*, *5*(June), 100064. https://doi.org/10.1016/j.memori.2023.100064

Saleem, M., Fang, L., Wakeel, A., Rashad, M., & Kong, C. Y. (2012). Simple Preparation and Characterization of Nano-Crystalline Zinc Oxide Thin Films by Sol-Gel Method on Glass Substrate. *World Journal of Condensed Matter Physics*, *02*(01), 10–15. https://doi.org/10.4236/wjcmp.2012.21002

Salwan K. Al-Ani. (2008). Methods of Determining The Refractive Index of Thin Solid Films. *J. of Appl. Phys.*, *4*(1), 17–23.

Sharmin, A., Tabassum, S., Bashar, M. S., & Mahmood, Z. H. (2019). Depositions and characterization of sol–gel processed Al-doped ZnO (AZO) as transparent conducting oxide (TCO) for solar cell application. *Journal of Theoretical and Applied Physics*, *13*(2), 123–132. https://doi.org/10.1007/s40094-019-0329-0

Shweta, K. P., & Thapa, K. B. (2019). Synthesis and characterization of ZnO nano-particles for solar cell application by the cost effective co-precipitation method without any surfactants. *AIP Conference Proceedings*, *2142* (September). https://doi.org/10.1063/1.5122336

Stroescu, H., Nicolescu, M., Mitrea, D., Tenea, E., Atkinson, I., Anastasescu, M., Calderon-Moreno, J. M., & Gartner, M. (2023). Effect of Al Incorporation on the Structural and Optical Properties of Sol–Gel AZO Thin Films. *Materials*, *16*(9). https://doi.org/10.3390/ma16093329

Tanaka, K., and Kato, M. (2024). Carrier recombination in highly Al doped 4H-SiC: dependence on the injection conditions. *Japanese Journal of Applied Physics*, *63*(1), 011002.

Tuan, P. (2023). Reduction of graphene oxide (go) to reduced graphene oxide (rgo) at different hydrothermal temperatures and enhanced photodegradation of zinc oxide/rgo composites. Physica Scripta, 99(1), 015912.

Üzar, N. (2024). Enhancement of structural, optical, electrical, optoelectronic and thermoelectric properties of ZnO thin film via Ni doping and Ni-B co-doping. Physica Scripta, 99(7), 075995.

Wang, Z., Zhang, X., Li, G., & Yu, B. (2016). Defect passivation in ZnO:Al:B thin films by post-annealing treatment. Journal of Physics D: Applied Physics, 49(10), 105101

Zhang, J., Liu, H.J., Wang, Z. R. and Ming, N. B.(2011) "Hydrothermal synthesis of ZnO nanorods and their optical properties," Journal of Crystal Growth, vol. 314(1) 76-80.